

REPORT DOCUMENTATION PAGE			Form Approved OMB NO. 0704-0188		
<p>The public reporting burden for this collection of information is estimated to average 1 hour per response, including the time for reviewing instructions, searching existing data sources, gathering and maintaining the data needed, and completing and reviewing the collection of information. Send comments regarding this burden estimate or any other aspect of this collection of information, including suggestions for reducing this burden, to Washington Headquarters Services, Directorate for Information Operations and Reports, 1215 Jefferson Davis Highway, Suite 1204, Arlington VA, 22202-4302. Respondents should be aware that notwithstanding any other provision of law, no person shall be subject to any penalty for failing to comply with a collection of information if it does not display a currently valid OMB control number.</p> <p>PLEASE DO NOT RETURN YOUR FORM TO THE ABOVE ADDRESS.</p>					
1. REPORT DATE (DD-MM-YYYY) 20-11-2014		2. REPORT TYPE MS Thesis		3. DATES COVERED (From - To) -	
4. TITLE AND SUBTITLE Acoustic Characterization of Grass-cover Ground				5a. CONTRACT NUMBER W911NF-09-1-0082	
				5b. GRANT NUMBER	
				5c. PROGRAM ELEMENT NUMBER 633606	
6. AUTHORS Chelsea E. Good.				5d. PROJECT NUMBER	
				5e. TASK NUMBER	
				5f. WORK UNIT NUMBER	
7. PERFORMING ORGANIZATION NAMES AND ADDRESSES The Catholic University of America Office of Sponsored Programs 620 Michigan Ave, NE Washington, DC 20064 -0001				8. PERFORMING ORGANIZATION REPORT NUMBER	
9. SPONSORING/MONITORING AGENCY NAME(S) AND ADDRESS (ES) U.S. Army Research Office P.O. Box 12211 Research Triangle Park, NC 27709-2211				10. SPONSOR/MONITOR'S ACRONYM(S) ARO	
				11. SPONSOR/MONITOR'S REPORT NUMBER(S) 55997-CS.6	
12. DISTRIBUTION AVAILABILITY STATEMENT Approved for public release; distribution is unlimited.					
13. SUPPLEMENTARY NOTES The views, opinions and/or findings contained in this report are those of the author(s) and should not be construed as an official Department of the Army position, policy or decision, unless so designated by other documentation.					
14. ABSTRACT  A custom designed acoustic impedance tube was used to measure acoustic properties of nonconsolidated materials, specifically soils and grass-covered ground. The tube was configured vertically for studying acoustic properties of granular materials i.e. soil and dirt. Software was developed to collect data and calibrate the impedance tube. An equivalent fluid model for describing sound propagation in rigid frame porous media was used to model acoustic behavior of dry and wet soils as well as grass covered and uncovered ground. The model requires six parameters:					
15. SUBJECT TERMS acoustic material property characterization, impedance tube, porous acoustic materials					
16. SECURITY CLASSIFICATION OF:			17. LIMITATION OF ABSTRACT	15. NUMBER OF PAGES	19a. NAME OF RESPONSIBLE PERSON
a. REPORT UU	b. ABSTRACT UU	c. THIS PAGE UU			Joseph Vignola
					19b. TELEPHONE NUMBER 202-319-6132

## **Report Title**

Acoustic Characterization of Grass-cover Ground

### **ABSTRACT**

A custom designed acoustic impedance tube was used to measure acoustic properties of nonconsolidated materials, specifically soils and grass-covered ground. The tube was configured vertically for studying acoustic properties of granular materials i.e. soil and dirt. Software was developed to collect data and calibrate the impedance tube. An equivalent fluid model for describing sound propagation in rigid frame porous media was used to model acoustic behavior of dry and wet soils as well as grass-covered and -uncovered ground. The model requires six parameters, i.e. porosity, tortuosity, flow resistivity, thermal permeability and viscous and thermal characteristic lengths. are measured separately. While flow resistivity was measured, the remaining five parameters were found by fitting procedure (optimization process). Theoretical models of sound propagation in porous media and acoustic measurements were used to explore the effects of water and vegetation (grass blades and roots) on the sound absorption and reflection of grass-covered ground. The acoustic and flow resistivity measures show that there is minute differences between the acoustic-soil interaction behavior between a root substrate with and without grass. Particularly with the soil samples, moisture encouraged broadband absorption in the higher frequency limits of the acoustic impedance measurements system compared to dried soil.

THE CATHOLIC UNIVERSITY OF AMERICA

Acoustic Characterization of Grass-cover Ground

A THESIS

Submitted to the Faculty of the  
Department of Mechanical Engineering  
School of Engineering  
Of The Catholic University of America  
In Partial Fulfillment of the Requirements  
For the Degree  
Master of Science

By

Chelsea Good

Washington, D.C

2014

## Acoustic Characterization of Grass-cover Ground

Chelsea Good, M.S.

Directed by: Joseph F. Vignola, Ph.D.

A custom designed acoustic impedance tube was used to measure acoustic properties of nonconsolidated materials, specifically soils and grass-covered ground. The tube was configured vertically for studying acoustic properties of granular materials i.e. soil and dirt. Software was developed to collect data and calibrate the impedance tube. An equivalent fluid model for describing sound propagation in rigid frame porous media was used to model acoustic behavior of dry and wet soils as well as grass-covered and -uncovered ground. The model requires six parameters, i.e. porosity, tortuosity, flow resistivity, thermal permeability and viscous and thermal characteristic lengths. are measured separately. While flow resistivity was measured, the remaining five parameters were found by fitting procedure (optimization process). Theoretical models of sound propagation in porous media and acoustic measurements were used to explore the effects of water and vegetation (grass blades and roots) on the sound absorption and reflection of grass-covered ground. The acoustic and flow resistivity measures show that there is minute differences between the acoustic-soil interaction behavior between a root substrate with and without grass. Particularly with the soil samples, moisture encouraged broadband absorption in the higher frequency limits of the acoustic impedance measurements system compared to dried soil.

This thesis by Chelsea Good fulfills the thesis requirement for the master's degree in Mechanical Engineering approved by Joseph F. Vignola, Ph.D., as Director, and by Diego Turo, Ph.D., and John Judge, Ph.D. as Readers.

---

Joseph F. Vignola, Ph.D., Director

---

Diego Turo, Ph.D., Reader

---

John Judge, Ph.D., Reader

## TABLE OF CONTENTS

	<b>Page</b>
<b>LIST OF FIGURES</b> .....	<b>v</b>
<b>LIST OF TABLES</b> .....	<b>vii</b>
<b>ACKNOWLEDGMENTS</b> .....	<b>viii</b>
 <b>CHAPTER</b>	
<b>1. INTRODUCTION</b> .....	<b>1</b>
1.1 Problem Statement, Approach and Contributions .....	2
<b>2. ACOUSTIC PROPERTIES OF POROUS MEDIA</b> .....	<b>3</b>
2.1 Equivalent fluid models .....	4
2.2 Single Parameter Model .....	5
2.3 JCAL Model .....	6
<b>3. ACOUSTIC MEASUREMENT SYSTEMS</b> .....	<b>9</b>
3.1 Impedance Tube Measurement System .....	9
3.1.1 Impedance Tube Theory .....	11
3.1.2 Validation of the Impedance Tube Measurements .....	12
3.1.3 Calibration of an Impedance Tube .....	14
3.2 Flow Resistivity Measurement System .....	14

<b>4. EXPERIMENT DESCRIPTION .....</b>	<b>17</b>
4.1 Samples .....	17
4.1.1 Sample Preparation .....	17
4.2 Measurement Parameters .....	19
4.3 Post processing of the data and fitting procedure.....	19
<b>5. RESULTS .....</b>	<b>20</b>
5.1 Flow Resistivity and Extracted Parameters .....	20
5.2 Moisture Effects in Soils .....	22
<b>6. CONCLUSION .....</b>	<b>28</b>
6.0.1 Future Work .....	28
<b>BIBLIOGRAPHY .....</b>	<b>29</b>

## LIST OF FIGURES

Figure	Page
3.1 The vertical impedance tube is shown has three sections. The top section holds a speaker that introduces sound into the next section which is hollow and has three ports for 1/2" microphones near the sample section. Ten identical simple sections were constructed for this study so that samples could be prepared and tested without disturbing their structure. ....	10
3.2 Theoretical Impedance Tube Diagram: the tube is vertically orientated and hardware that consists of a speaker, two microphones, and sample with a rigid back. The speaker propagates a sound signal which is reflected by the sample and record by the microphones. ....	11
3.3 (Top) Reflection and (Bottom) Absorption coefficient of blue sand. Sample thickness is equal to 5cm, $\phi = 0.41$ , particle radius $r = 250 \mu m$ . Gray circles are impedance tube data. Black line is the JCAL model with parameters estimated using the cell model .....	13
3.4 Left: Flow resistivity measurement system consisting of air compressor, pressure regulator, flow meter, sample holder, and a Dwyer vertical inclined manometer Center: aluminum calibration cylinder with single 0.25 in pore Right: shows tight fitting of the cylinder to the tube walls .....	15
4.1 The sample grow box is show. On the right side is germinated kentucky perennial grass. On the left side soil that has been sieved to 4.75 mm grain size. The 4 inch grid system marks each sample to be cut .....	18
5.1 The flow resistivity measurements of all the grass samples. The flow resistivity is based on the slope of the flow resistivity as it varies with velocity. ....	21
5.2 The flow resistivity measurements of all the root samples. ....	22



5.3	The grass sample that weighed 145.6g, root-ground substrate was 4.4 cm thick and had a moisture content of 36.1%. The grass sample is fitted to the JCA, Delany-Bazley, and Miki models. ....	24
5.4	The root samples weighed 145.6g, root-ground substrate was 4.4 cm thick and had a moisture content of 36.1%. The moist root sample is fitted to the JCA, Delany-Bazley, and Miki models .....	25
5.5	The soil sample weighed 86.8 g after dissication. The sample was 2.9 cm thick. The moist and dry soil samples' acoustic impedance data were fitted to the JCA model .....	26

## LIST OF TABLES

Table	Page
3.1 Sand parameters estimated using cell model .....	13
4.1 Excitation Parameters .....	19
5.1 Physical and Extracted Parameters of Each Sample .....	27

## **ACKNOWLEDGMENTS**

I would like to express my appreciation to all those who aided in the idea, research, and collection of data for this thesis work. I am especially grateful for the for my professors and mentor for without whose encouragement and aid I would not have made it this far in my research.

# **CHAPTER 1**

## **INTRODUCTION**

Research at CUA using a side scanning synthetic aperture acoustic imaging device in outdoor settings presented an issue that needed investigation. In these measurements, sound was projected at targets and backscattered sound was recorded. Targets lying in grassy terrain, regardless of sound energy or frequency range, become difficult to detect using the imaging system. This realization motivated research to understand the cause of these effects. This thesis describes an experimental study of samples of isolated soil, grass with root substrate, and sheared root substrate under both wet and evaporated conditions. These measurements were used to characterize sound absorption from grass and soil under various conditions.

Soil itself is a porous medium, consisting of solid matter and voids that can contain air or water. Characterization of porous media has a history dating at least to 1961 with the work of Biot [1]. This subject of research has continued over the past 50 years [2]; however, specifically characterizing grasses and soil interactions with sound measurements has yet to be thoroughly investigated. Recently, Horoshenko [3] measured the acoustic properties of low growing plants where he primarily focused on measuring the effects of density, surface area, and orientation of the plants' leaves. During this experiment, Horoshenkov removed the roots from the ground and investigated the ground and plant system separately. The present work builds from Horoshenkov by using similar measurement techniques and treating the grass substrate as single system consisting of roots that secure the plant to the ground and draw moisture up to the

plant. The complete structure has a consolidating effect on the soil and the presence of the roots reduce the effective porous volume.

Acoustic impedance soil surface has been studied since 1961 [4] and many authors have created different methods and models to characterize outdoor sound propagation on grass-covered ground. The first study on living grass using an impedance tube was conducted by Dickinson and Doak in 1970 [5]. Then a model that accounted for porosity change with depth was proposed in by Donato in 1977 [6]. Most recently Attenborough [7] wrote a review about outdoor ground impedance models and compared predictions of sound absorption to those models with data. He found that a phenomenological model fit data better than widely used simple models like the single parameter approach given by Delany-Bazley [8].

## **1.1 Problem Statement, Approach and Contributions**

This work seeks to understand the reflection and absorption characteristics of soil with foliage and roots and thus their effect on the quality of acoustic images. Indoor experiments are used to characterize representative samples consisting of grass blades, root systems, and soil using an impedance tube. Acoustic data collected on the samples was compared to existing theoretical models. These results provide an understanding of issues related to this complex outdoor imaging technique. This work presents findings from 6 samples under 2 different conditions (moist and dry) showing frequency dependent absorption of sound. In addition, air flow resistance of each sample was measured in order to better estimate the physical parameters required for the theoretical models, enabling comparison to the theoretical models.

Ultimately this yields parameters that describe the reflection and absorption behavior of the composite. The work consists of a set of measurements, a comparison of the measurements to pre-existing models, and the development of a new parametric model accounting for moisture content.

## **CHAPTER 2**

### **ACOUSTIC PROPERTIES OF POROUS MEDIA**

Porous media have been a subject of interest because of their ability for noise and reverberation control. Examples of porous media are cements, ceramics, rocks, building insulation, foams and soil. Characterizing the acoustical properties of these materials is challenging due to their complex structures and requires knowledge of several physical attributes. These physical attributes are the material's porosity, permeability, tortuosity, flow resistivity, and both the viscous and thermal characteristic lengths. Most of these are difficult to independently measure. Predictive models have been developed by Biot [1], Delany and Bazley [9], Johnson et al. [10], and Wilson [11] for rigid porous materials. The most effective way to account for dissipation of sound in porous media is to model a medium with an equivalent fluid where the wavenumber and characteristic impedance are expressed as complex quantities.

The simplest equivalent fluid models were proposed by Delany and Bazley [9] and Miki [12]. Their models require only one parameter, i.e. flow resistivity, and were successful for predicting the characteristic impedance and wavenumber of porous media with highly porous materials like fibrous structures. However, these models are were proven to be inaccurate for materials with low porosity like the majority of granular materials.

The most robust and widely used equivalent fluid model were developed in the last decades by Johnson et al. [10], Champoux and Allard[13], and Lafarge[14]. This model, commonly called the JCAL model (from the initials of its authors) uses six physical parameters that can

be measured independently by using non-acoustical tests. The six physical parameters consist of porosity, tortuosity, flow resistivity, thermal permeability and viscous and thermal characteristic lengths. Five of these are difficult to physically measure, however, flow resistivity can be measured with the proper measurement system.

## 2.1 Equivalent fluid models

Momentum and mass conservation equations for plane wave propagation in the  $x$ -axis in a lossless fluid can be formulated in the frequency domain as follows

$$-i\omega p = -K \frac{\partial u}{\partial x} \quad (2.1)$$

$$-i\omega \rho_o u = -\frac{\partial p}{\partial x} \quad (2.2)$$

In Eqs. 2.1 and 2.2,  $p$  is the acoustic pressure,  $u$  is the particle velocity,  $K$  is the bulk modulus of the fluid ( $K = \rho_o c^2$  speed of sound in the fluid), and  $\rho_o$  is the density of the fluid. Bulk modulus and density are real constants. In most common free field applications, air is considered as lossless fluid and Eqs. 2.1 and 2.2 can be applied without approximations. However, when acoustic waves travel in narrow channels (much smaller than the acoustic wavelength) viscous and thermal losses occur in proximity of the walls of those channels. For traveling waves in channels, the governing equations will now be written as

$$-i\omega p = -K(\omega) \frac{\partial u}{\partial x} \quad (2.3)$$

$$-i\omega \rho(\omega) u = -\frac{\partial p}{\partial x} \quad (2.4)$$

where density  $\rho(\omega)$  and bulk modulus  $K(\omega)$  are now frequency dependent complex quantities because of viscous and thermal losses. A rigid frame porous media can be modeled as a network of channels or pores and sound propagating through this medium can be described as

$$-i\omega\phi p = -K(\omega)\frac{\partial u}{\partial x} \quad (2.5)$$

$$-i\omega\rho(\omega)u = -\phi\frac{\partial p}{\partial x} \quad (2.6)$$

where  $\phi$  is the porosity of the medium. Porosity, a real constant, is the ratio between the volume of the pores (filled with air) and the total volume of the porous medium. For this analysis, sound speed,  $c$  and wavenumber,  $\Gamma$  in a porous media need to be defined. These complex quantities are given as

$$c = \sqrt{\frac{K(\omega)}{\rho(\omega)}} \quad (2.7)$$

$$\Gamma = \omega\sqrt{\frac{\rho(\omega)}{K(\omega)}} \quad (2.8)$$

## 2.2 Single Parameter Model

The complex wavenumber,  $\Gamma$  and the characteristic impedance,  $Z_c$  for many fibrous materials with porosity close to 1 were measured by Delany and Bazley[15] in 1970 over a wide range of frequencies. They found that the complex wavenumber and characteristic impedance depended mainly on the excitation frequency and the static flow resistivity,  $\sigma_o$  of the material. This static flow resistivity is a measure of the resistance of the material to the flow of air through it.

Delany and Bazley proposed the following empirical expression for  $\Gamma$  and  $Z_c$ :

$$Z_c = \rho_o c \sqrt{\frac{\alpha_\infty}{\phi}} \left( 1 + 0.0571X^{-0.754} - j0.087X^{-0.732} \right) \quad (2.9)$$

$$\Gamma = \frac{\omega}{c} \sqrt{\alpha_\infty} \left( 1 + 0.0978X^{-0.7} - j0.0189X^{-0.595} \right) \quad (2.10)$$



where  $\rho_o$  and  $c$  are the air density and the speed of sound in air and  $X$  is a dimensionless parameter

$$X = \frac{\rho_o \omega}{2\pi \sigma_0} \quad (2.11)$$

For these empirical expressions to be valid, the authors suggested that  $0.01 < X < 1$ . These boundaries can be seen as frequency limits for a given material. The Delany and Bazley model does not provide a perfect prediction of acoustic behavior of all porous materials in the frequency range previously defined. Nevertheless, these expressions are widely used and can provide reasonable approximations for  $\Gamma$  and  $Z_c$ .

A slightly different empirical expressions for  $\Gamma$  and  $Z_c$  proposed by Miki[12] are:

$$Z_c = \rho_0 c_0 \left( 1 + 0.0571X^{-0.754} - j0.087X^{-0.732} \right) \quad (2.12)$$

$$\Gamma = \frac{\omega}{c_0} \left( 1 + 0.109X^{-0.618} - j0.160X^{-0.618} \right) \quad (2.13)$$

This model also applies in the frequency range  $0.01 < X < 1$ .

Horshenkov *et al.*[3] showed recently that this model is able to provide satisfactory predictions of the fundamental acoustic properties of foliage and soils. However, in addition to the flow resistivity data, the model used by this group relies on the data which was measured directly and linked to the morphology of a specific plant.

### 2.3 JCAL Model

Acoustic behavior of rigid frame porous materials can also be described by the JCAL model[10]. In this model complex density and bulk modulus are functions of angular frequency and six physical parameters. Their expressions are as follows:

$$\rho(\omega) = \rho_0 \left( \alpha_\infty + \frac{\sigma_0 \phi}{-i\omega \rho_0} \sqrt{1 - i\omega \frac{\eta}{\rho_0} \left( \frac{2\rho_0 \alpha_\infty}{\sigma \phi \Lambda} \right)^2} \right) \quad (2.14)$$

$$K(\omega) = \rho_0 c_0^2 \left( \frac{\gamma - 1}{1 + \frac{\eta \phi}{-i\omega \rho_0 N_{Pr} k'_0} \sqrt{1 - \frac{i\omega \rho_0 N_{Pr}}{\eta} \left( \frac{2k'_0}{\phi \Lambda'} \right)^2}} \right)^{-1} \quad (2.15)$$

where  $\alpha_\infty$  is tortuosity,  $\phi$  is porosity,  $\Lambda$  is viscous characteristic length,  $\sigma_0$  is static flow resistivity,  $\eta$  dynamic viscosity of air,  $\Lambda'$  is thermal characteristic length,  $k_0$  is thermal permeability,  $N_{Pr}$  is Prandtl number. Tortuosity values larger than 1 indicate that sound waves have to travel through a tortuous path while crossing the medium. Viscous loss increases with greater tortuosity. Characteristic viscous length is equivalent to the hydraulic radius but for more general microgeometries. The static flow resistivity is proportional to the inverse of viscous permeability  $k_0 = \frac{\eta}{\sigma_0}$ . Characteristic thermal length and thermal permeability are thermal equivalents to the characteristic viscous length and permeability. Characteristic impedance  $Z_c$  and complex wavenumber  $\Gamma$  can therefore be evaluated:

$$Z_c = \frac{1}{\phi} \sqrt{\rho(\omega) p(\omega)} \quad (2.16)$$

$$\Gamma = \omega \sqrt{\frac{\rho(\omega)}{K(\omega)}} \quad (2.17)$$

The main advantage of this model is that it works for any frequency range and porosity value.

Ground surfaces of low porosity may be considered acoustically hard according to Attenborough [16] [7], and vegetation covered ground is to be considered acoustically soft. In general, porous ground surfaces are elastic as well as porous and their elastic response may be significant at high amplitude and low frequency noise. But, for more typical noise predictions such as for noise from surface transport, the choice of impedance models can be confined to those representing the acoustical properties of airfilled porous materials with rigid frames [7].

Under these circumstances the JCAL model can predict and describe the acoustic behavior of grass covered ground with good approximation. However, determination of six parameters is needed. For the purpose of exploring the acoustic effects of the water, grass blades and roots on reflection and absorption coefficient of grass covered ground, comparisons between multiple experiments performed on dry and wet soil and grass covered and uncovered ground can be used. Then optimization procedures can be used to fit the JCAL model to the data and estimate the unknown parameters of the model. The determination of those parameters will be used for interpreting the data.

## **CHAPTER 3**

### **ACOUSTIC MEASUREMENT SYSTEMS**

#### **3.1 Impedance Tube Measurement System**

An impedance tube is an instrument used to measure the surface impedance and reflection coefficient of sound absorbing material for plane waves at normal incidence. An impedance tube can be either a circular or square cross-section duct with an acoustic source mounted at one end. For the system used in this study the source is an audio speaker which broadcasts an acoustic excitation through the tube toward a sample of material. This sample is mounted on a rigid termination located on the opposite end of the tube. The acoustic excitation signal launched from the speaker propagates as a plane wave to the sample where it is both reflected and absorbed. Two microphones placed between the speaker and sample each measure the acoustic pressures of both the waves incident to and reflected by the sample. The two microphone signals are used to determine surface impedance and reflection coefficient of a sampled material using the transfer function method.

In order to perform measurements on unconsolidated porous media similar to soil, a vertical impedance tube as shown in Fig. 3.1 was designed and built at the acoustic and vibration lab of the CUA. It was designed in accordance with ASTM E 1050-98. Its size and microphone spacing allow for an operating frequency range of 200 - 2000 Hz. The tube is made of aluminum pipe with a 3.5 in. (88.9 mm) inner diameter and a 4.5 in. (114 mm) outer diameter. The entire tube is 34 in. (86.5 cm) long. The tube consists of two sections, which are

held together outside the tube with cam latches. The samples are inserted into a base section of the tube when the tube is unlatched. At the top of the instrument section of the tube is a 75 mm (2.95 in.) audio speaker and at the bottom are two 1/2 inch (12 mm) B&K 4165 microphones. Three microphone ports are located 44.4, 107.8, or 177.8 mm from the joint, which hold the microphones so that the microphone tip is flush with the inner surface of the tube.



Figure 3.1: The vertical impedance tube is shown has three sections. The top section holds a speaker that introduces sound into the next section which is hollow and has three ports for 1/2" microphones near the sample section. Ten identical simple sections were constructed for this study so that samples could be prepared and tested without disturbing their structure.

Impedance tubes are used to measure sound transmission loss through a sampled material based on the transfer function method. The reflected and incident energies are (pressures sensed at each pass of the mic) evaluated with the transfer function method to extract acoustic properties of each sampled material. The tube is excited by a Kenwood KFC 835C speaker driven by a Krohn-Hite 7600 power amplifier. A National Instruments 6259 DAQ controlled by LabView is used as the signal source and to record the measured data. The two acoustic

pressures are measured by the 1/2 in (12.8 mm) B&K 4165 microphones, which are powered by a B&K 5935 pre-amplifier.

### 3.1.1 Impedance Tube Theory

The complex acoustic pressure measured at each microphone position is the superposition of the incident and reflected waves as seen in Fig. The pressure is recorded at two locations by

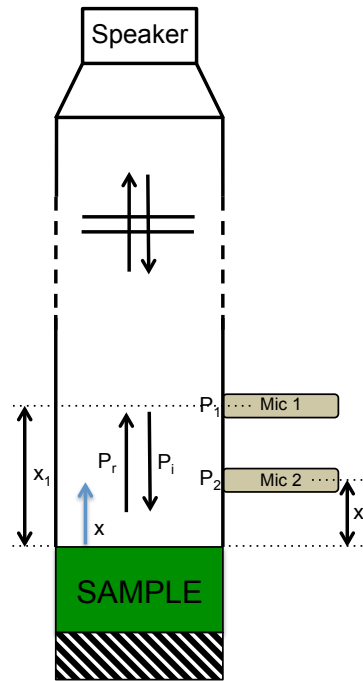


Figure 3.2: Theoretical Impedance Tube Diagram: the tube is vertically orientated and hardware that consists of a speaker, two microphones, and sample with a rigid back. The speaker propagates a sound signal which is reflected by the sample and record by the microphones.

the two microphones. A transfer function,  $H_{12}$ , is formed with the pressure measurements.

$$H_{12} = \frac{P_2(\omega)}{P_1(\omega)} = \frac{P_i e^{jk_0 x_2} + R(\omega) P_i e^{-jk_0 x_2}}{P_i e^{jk_0 x_1} + R(\omega) P_i e^{-jk_0 x_1}} \quad (3.1)$$

In Eq. 3.1,  $P_1$  and  $P_2$  are the acoustic pressures measured at each respective microphone,  $P_i$  is the incident pressure,  $k_0$  is wave number in air,  $\omega$  is angular frequency,  $x_1$  and  $x_2$  are the dis-

tances between the sample surface and microphone. The reflection and absorption coefficients,  $R(\omega)$  and  $\alpha$  respectively of the sample are calculated using the transfer function with Eqs. 3.2 and 3.3 respectively [17] [18].

$$R(\omega) = \frac{e^{jk_0^{x_1-x_2}} - H_{12}}{H_{12} - e^{jk_0^{x_1-x_2}}} e^{2jk_0x_1} \quad (3.2)$$

This calculation gave us the reflection coefficient, Allard gives an expression for the absorption coefficient as:

$$\alpha(\omega) = 1 - R(\omega)^2 \quad (3.3)$$

In addition, Allard gives an expression for surface Impedance,  $Z_s(\omega)$

$$Z_s(\omega) = \rho c \frac{1 + R(\omega)}{1 - R(\omega)} \quad (3.4)$$

where  $\rho$  is the density of air, and  $c$  is the sound speed of air.

### 3.1.2 Validation of the Impedance Tube Measurements

Blue aquamarine sand with grain diameters ranging from 500-600  $\mu\text{m}$  was used to confirm accurate measurement of the system. Packed spherical particles have acoustic properties that demonstrate the effect of interstitial space within the material; interstitial spacing allows for the sound to become trapped between the spheres. The cell model was used for estimating the acoustic parameters of sand [19] [20]. This theoretical model can estimate  $\sigma$ ,  $k'_0$ ,  $\Lambda$ ,  $\Lambda'$  and  $\alpha_\infty$  of spherical particles as long as the radius  $r$  and porosity are known. A sample containing 5 cm of loosely packed blue aquamarine sand had  $r = 250 \mu\text{m}$  and porosity  $\phi = 0.41$ . Based on the cell model the parameters shown in Table 3.1 were estimated.

$r$ ( $\mu\text{m}$ )	$\phi$	$\alpha_\infty$	$\sigma$ ( $\text{kPa s/m}^2$ )	$\Lambda$ ( $\mu\text{m}$ )	$k'_0$ ( $\text{nm}^2$ )	$\Lambda'$ ( $\mu\text{m}$ )
250	0.41	1.72	65.8	79.9	69.2	115.8

Table 3.1: Sand parameters estimated using cell model

The parameters were then used in the Johnson-Champoux-Allard-Lafarge (JCAL) model expressed as Eqs. 2.14 and 2.15. An acoustic impedance tube measurement of the blue aqua-marine sand was performed to determine reflection and absorption coefficients. Characteristic impedance and wavenumber were evaluated using Eqs. 2.16 and 2.17. The JCAL model fit with the data Fig. 3.3 showing that the system provides reliables measurements.

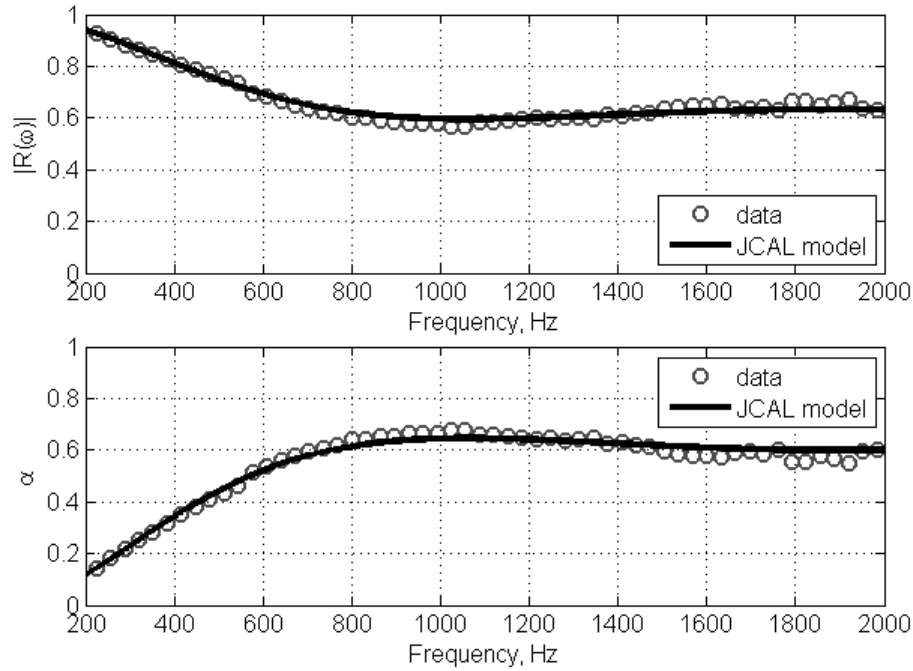


Figure 3.3: (Top) Reflection and (Bottom) Absorption coefficient of blue sand. Sample thickness is equal to 5cm,  $\phi = 0.41$ , particle radius  $r = 250 \mu\text{m}$ . Gray circles are impedance tube data. Black line is the JCAL model with parameters estimated using the cell model



### 3.1.3 Calibration of an Impedance Tube

The impedance tube needs to be calibrated before any set of measurements in order to account for microphone phase mismatch. To perform the calibration of the tube an absorbing material with known acoustic properties is used. A sample of Melamine foam, 5 cm thick was used to perform the calibration. The goal of the calibration measures is the estimation of a correction factor. All the transfer functions measured using the samples of interest will be multiplied by this factor to account for the phase mismatch between the microphones.

The impedance tube measurement system was calibrated using materials with known acoustic properties in order to confirm accurate measurement of the system. Melamine foam 5 cm (1.97 in.) in thickness was used to perform this calibration measurement. The calibration measures the correction factor which accounts for phase mismatch between the microphones.

## 3.2 Flow Resistivity Measurement System

Flow Resistivity is the ratio of static pressure drop to volumetric flow through a porous material. The majority of porous media models are based on the knowledge of at least one parameter: the static flow resistivity. The static flow resistivity is a measure of the acoustic resistance or permeability of the material to the air flow. It plays an important role for describing the viscous loss that takes place during wave propagation inside the pores of the material. For this reason, a flow resistivity measurement system was designed and built according to ASTM Standard C522- 03 [21]. The flow resistivity measurement system consists of a controlled laminar flow through a sample and measuring the pressure difference across the sample. Most models describe fibrous materials whose porosity are close 1, however, for unconsolidated materials such as soils the flow resistivity needs to be measured. For this reason, a flow resistivity measurement system was built to measure the flow resistivity of each sample. The flow resistivity measurement system consists of a compressed air line, a flow meter, diffuser, and inclined

manometer. The compressed air line is restricted by the pressure regulator to only output 20 psi into the variable flow meter. Adjusting the flow meter across a range of 6 - 30 SCFH (cubic feet per hour) and recording the corresponding pressures from the manometer provides the flow resistivity (the relationship of the volumetric flow rate and the differential pressure drop through the sample). Calibration of the flow resistivity measurement system was conducted to

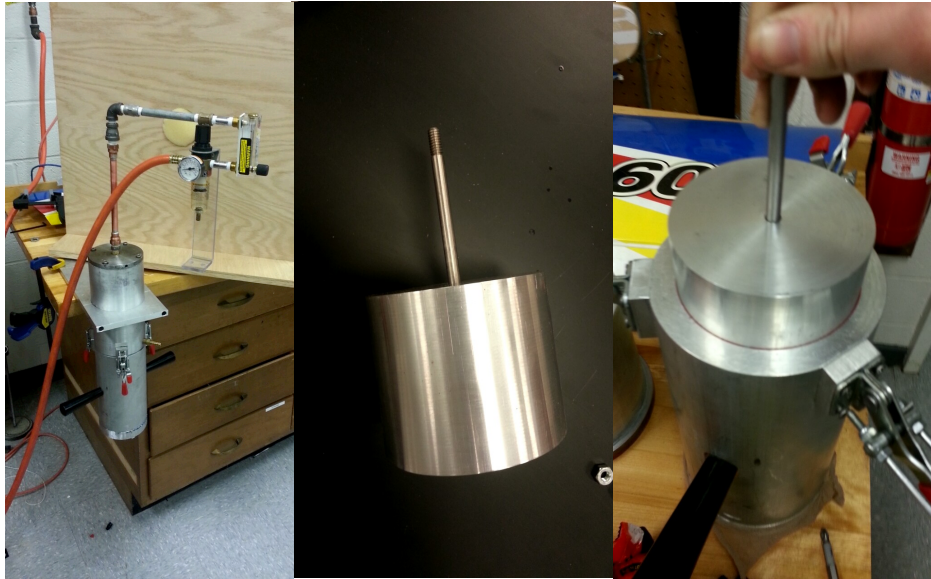


Figure 3.4: Left: Flow resistivity measurement system consisting of air compressor, pressure regulator, flow meter, sample holder, and a Dwyer vertical inclined manometer Center: aluminum calibration cylinder with single 0.25 in pore Right: shows tight fitting of the cylinder to the tube walls

confirm accurate readings. Fig. 3.4 shows photographs of an aluminum cylinder with a single 0.25 inch pore used for this calibration. The resistance of flow through a single pore is

$$R = \frac{\Delta P}{Q} = \frac{8\mu L}{\pi a^4} \quad (3.5)$$

where  $\Delta P$  is the change in pressure across the sample,  $Q$  is the volumetric flow rate,  $\mu$  is the dynamic viscosity of air ( $18.72e^{-6} \frac{kg}{sm}$ ),  $L$  is the thickness of the sample,  $a$  is the pore radius.

This expression can be modified to account of the a number of pores,  $N$  in the sample as follows.

$$R = \frac{8\mu L}{N\pi a^4} \quad (3.6)$$

## **CHAPTER 4**

### **EXPERIMENT DESCRIPTION**

#### **4.1 Samples**

##### **4.1.1 Sample Preparation**

The samples were encased in a 4 ft (122 cm) by 3 ft (91.4 cm) wooden box, as shown in Fig. 4.1. The Miracle-Grow fertilized soil was initially sieved with a ASTM E11 sieve to remove all rocks, bark, other organic matter. The sieve also ensured a grain size less than 4.75 mm in diameter. The soil is initially approximately 4 in (10.12cm) in depth when laid in the soil plot. Kentucky perennial grass seeds are spread over the half of the soil with approximately 40 seeds planted per square inch (6.45 m<sup>2</sup>). Over the course of 3 weeks the grass is grown until the height of each blade is 4 to 5 inches (10-13 cm).

The grass was kept indoors and kept at the indoor temperature of 72 degrees. It was grown from a seedling completely indoors while receiving exactly 6 hours of artificial sunlight from hydroponic grow lights. Each side of the sample plot was watered daily 1.25 L of tap water evenly spread using a watering can.

Prior to impedance tube measurement the samples were cut using a plunger cutter with a 3.5 in (88.9 cm) diameter. This ensures all the layers evenly fit the tube without air gaps between the substrate and the sample holder walls (vital to accurate impedance measurement). The samples were first placed in the flow resistivity rig where flow rate and pressure measurements were taken. The flow resistivity parameter was extrapolated from these measurements. The

sample holder was then attached by cam latched to the impedance tube. The weight of the moist samples within their respective holder was taken.

After the initial impedance tube measurements, the samples were dried, and the initial moisture content was estimated in accordance with ASTM C70-13 using the burn-off method. The impedance tube sample holders were placed into a oven set to 110° C and cooked for 24 hours removing nearly all the moisture within the sample. The dessicated samples were weighed and the moisture content was computed based on the weight difference. The dessicated samples were measured with the impedance tube for the second time, as dry specimens.



Figure 4.1: The sample grow box is show. On the right side is germinated kentucky perennial grass. On the left side soil that has been sieved to 4.75 mm grain size. The 4 inch grid system marks each sample to be cut

## 4.2 Measurement Parameters

Table 4.1: Excitation Parameters

Excitation Parameters	
Chirp Band	100-200 Hz
Chirp Duration	250 ms
Sampling Frequency	40 KHz
Microphone	$\frac{1}{4}$ in. B & K Model 4165 Mic
Sensitivity	50 mV/Pa

## 4.3 Post processing of the data and fitting procedure

Data fitting was achieved using a built-in Matlab function “fminsearch”. In this function a Nelder–Mead simplex direct search algorithm is implemented. In this study, “fminsearch” has been used to find a set of parameters that minimize the difference between a chosen model and the measured reflection coefficient at all frequencies. First the “Cell model” which uses of only two parameters, pore radius and porosity, was employed to fit the data. This simple model allows initializing the search of a multiple-variable model like the JCA model. The porosity and flow resistivity used for the JCA model were then used to initialize the parameter search of the Delany-Bazley and Miki models. Predicted parameters values of these models are tabled in table 5.5.

## **CHAPTER 5**

### **RESULTS**

#### **5.1 Flow Resistivity and Extracted Parameters**

For each moist sample, the flow resistivity was physically measured in a flow resistivity measurement system. The results are displayed in Figs. 5.1 and 5.2. The samples then underwent acoustic measurements in an impedance tube. These measurements uncover the sample characteristics. The combination of these acoustic characteristics and pre-existing theoretical models allows for estimation of other sample parameters. These extracted parameters provide further insight into the sample in its different states and its potential behavior with respect to sound propagation. Static flow resistivity is one of those parameters, which was both measured and estimated by model fitting for this experiment. Measured and estimated values of flow resistivity of grass samples reveal that the grass blades do not contribute to the flow resistivity of the sample. In Fig. 5.1 the flow resistivity is slightly lower than that of its root-substrate (without blades).

It is important to consider the way the sample thickness is evaluated. For example the sample thickness significantly influences the flow resistivity value. If the root-substrate and the blade height are combined, increasing the overall sample thickness there will be an underestimation of the flow resistivity. Both the physical measurements and the models reflect this result when the blades are considered a part of the sample thickness. It is possible to explain this phenomenon by the fact that between the cutting process and the replacement of the sam-

ple into the flow resistivity rig the pores structure might have been slightly modified. These results lead to the conclusion that the grass layer did not contribute to a significant increase of the flow resistivity and that their presence does not affect the absorption property of the soil.

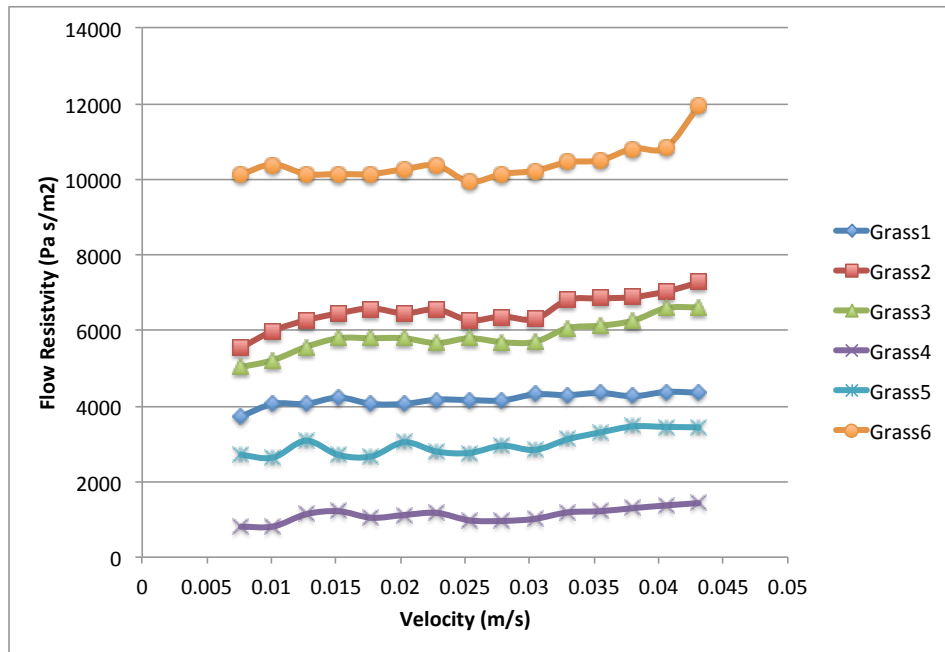


Figure 5.1: The flow resistivity measurements of all the grass samples. The flow resistivity is based on the slope of the flow resistivity as it varies with velocity.



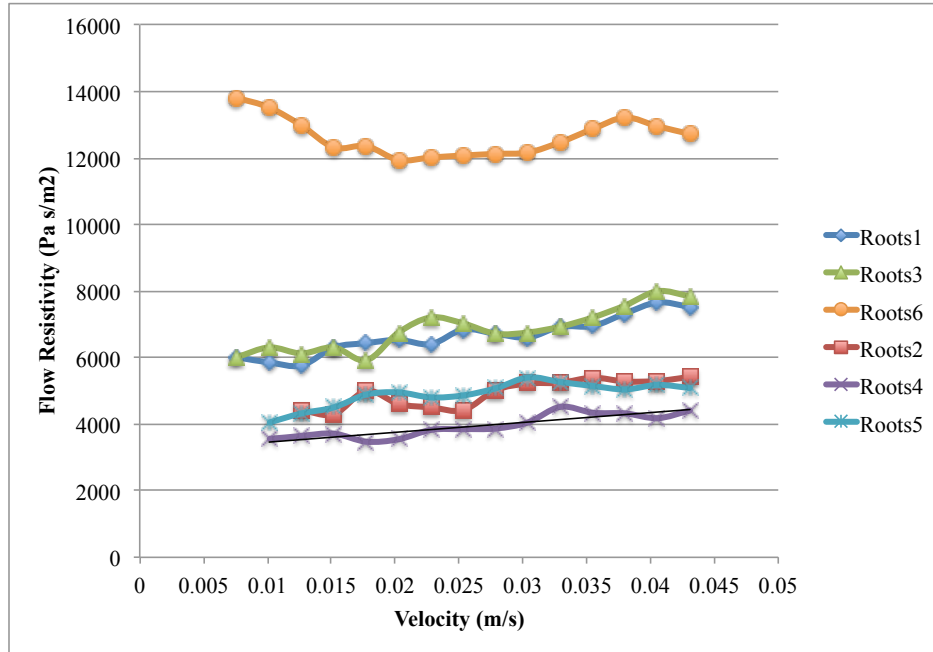


Figure 5.2: The flow resistivity measurements of all the root samples.

## 5.2 Moisture Effects in Soils

Wet samples were thicker than their dry counterpart. This cannot be simply justified by the absence of water in the dry sample. The amount of water in the sample, measured by weight difference, can only justify 27.6% reduction in volume or 1.1 cm in thickness of the dry sample. The remaining thickness reduction must be due to the collapse of the pore structure that occurred after the desiccation of the sample. The effects of these phenomena are observed through the parameters value predicted by the fitting of Delany-Bazley, Miki and JCA models to the absorption coefficient of the sample. In particular, only JCA and Delany-Bazley models predict a flow resistivity values that are in agreement with published data[ref Attenborough book] ( $\frac{kPa \cdot s}{m^2}$ ) and both show that flow resistivity decreases from wet to dry. However, the data fit shows that only JCA capture the acoustic behavior of both wet and dry samples. The JCA model reveals also that a wet sample has lower porosity compared to its dry equivalent,

which is expected since the water fills the pores, and that tortuosity. Thus reduction of flow resistivity and increase of porosity suggest that the pores in dry soil samples are narrower and numerous.

With the Johnson-Champoux-Allard model one can fit the averaged data curve and base the parameters values on the fitting. This model has been shown to be the most robust phenomenological model for sound absorption of rigid-frame porous media. It uses 6 independent parameters: Porosity, tortuosity, flow resistivity, thermal permeability, viscous and thermal characteristic lengths. There is better overall agreement between fitting curve and dry soil data compared to the wet soil data. This model is designed for porous filled with single phase fluid while in the case of soil the pores are filled with both air and water. In the "wet-data" some extra absorption is observed around 400-600 Hz which is not captured by the model as well as at frequency between 1700-2000 Hz "Dry-data" are well fitted by the model except for an extra absorption observed at around 200-300 Hz. We are not entirely sure about this, but the vibration of the superficial layer of the soil might be the cause of it.

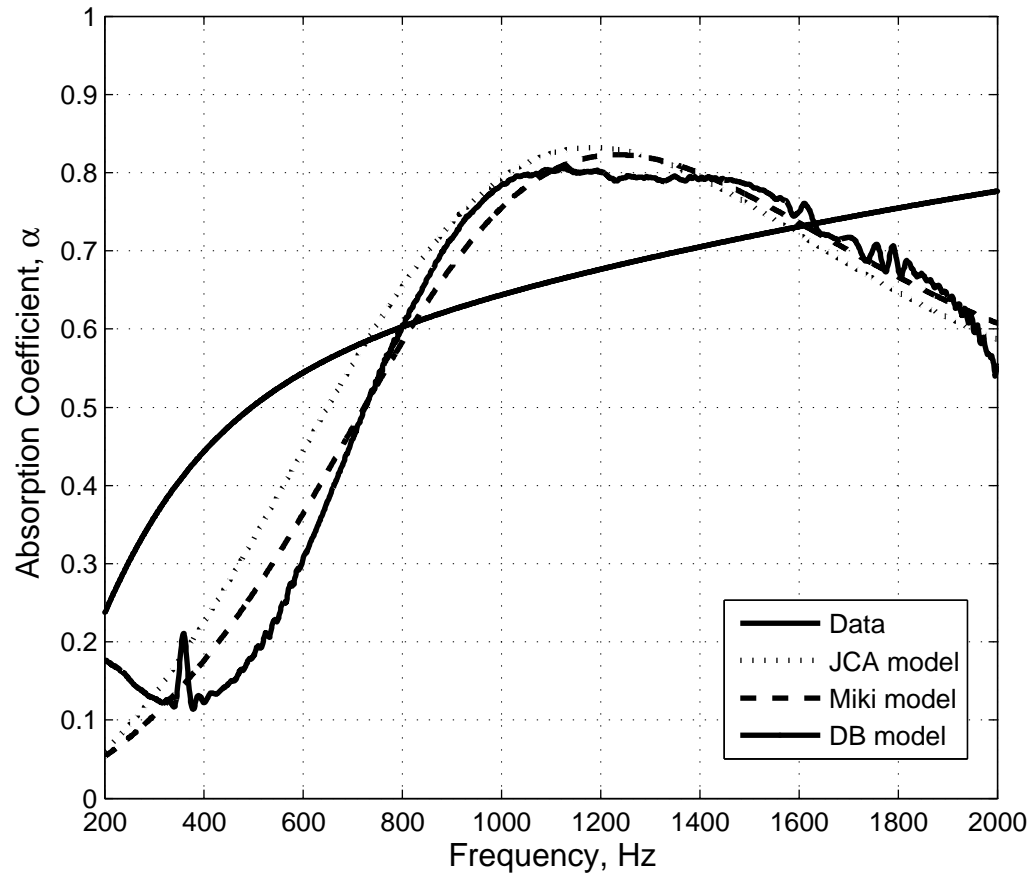


Figure 5.3: The grass sample that weighed 145.6g, root-ground substrate was 4.4 cm thick and had a moisture content of 36.1%. The grass sample is fitted to the JCA, Delany-Bazley, and Miki models.

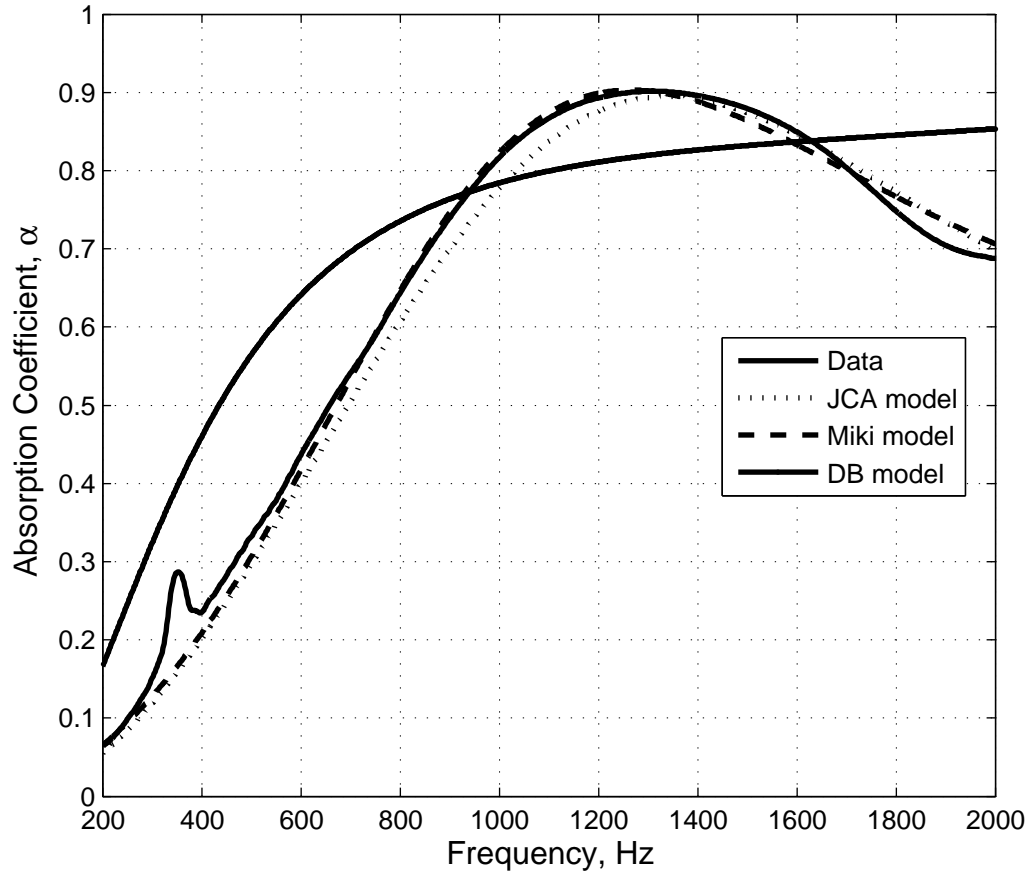


Figure 5.4: The root samples weighed 145.6g, root-ground substrate was 4.4 cm thick and had a moisture content of 36.1%. The moist root sample is fitted to the JCA, Delany-Bazley, and Miki models

JCA model fit in fig. 5.4 shows that wet soil with roots has lower flow resistivity ( $33.6 \frac{kPa \cdot s}{m^2}$ ) and lower porosity (0.38) than its dry counterpart ( $37 \frac{kPa \cdot s}{m^2}$ , 0.72 respectively). This was expected since the pores of the wet sample are partially filled with water reducing the porosity of the sample.

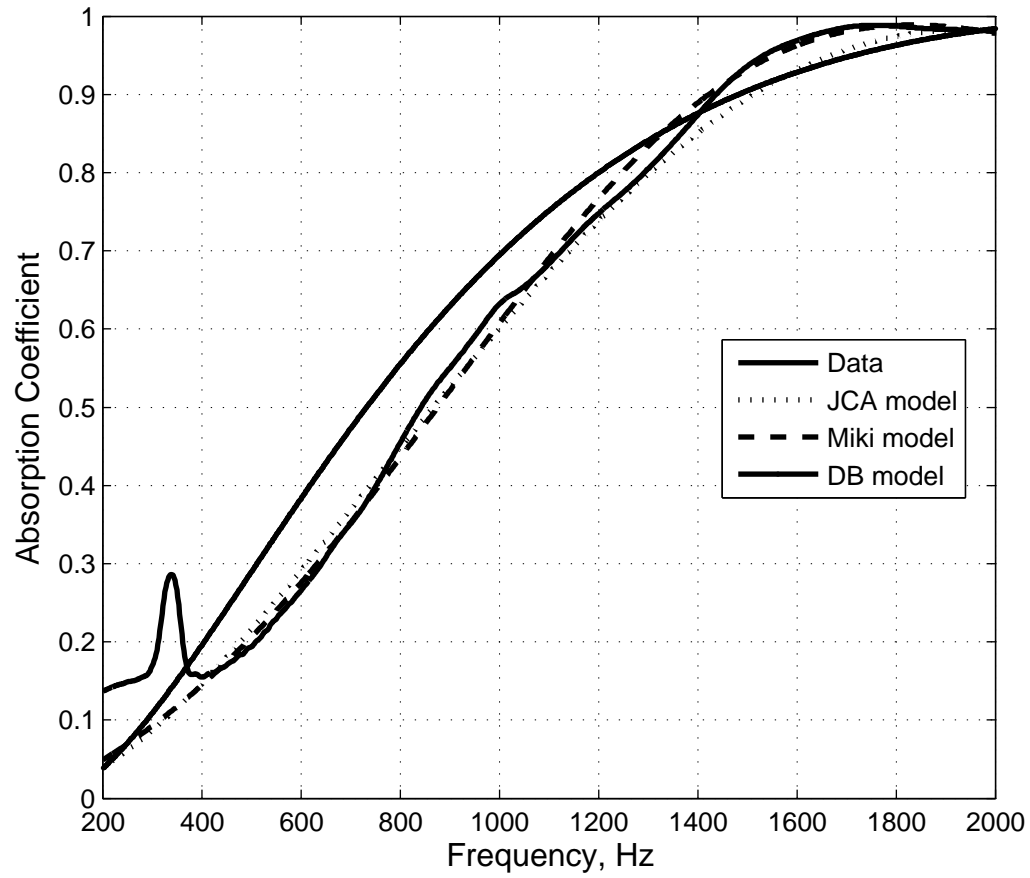


Figure 5.5: The soil sample weighed 86.8 g after dissication. The sample was 2.9 cm thick. The moist and dry soil samples' acoustic impedance data were fitted to the JCA model

Method	Parameters	Wet soil	Dry soil	Covered Grass soil	Wet soil with roots	Dry soil with roots
Direct	Thickness (cm)	4.1	3.3	2.5 + 4.4	4.4	2.9
	Water content (g)	70	0	50	50	0
	Water content (volume %)	27.6	0	5.5	5.5	0
	Eq. water thickness (cm)	1.1	0	0.8	0.8	0
	Flow resistivity	-	-	32.620	36.324	-
Cell model	Eq. radius (mm)	0.314	0.199	0.348772	0.397	8.12E-05
	Porosity	0.44	0.56	0.40	0.38	0.72
JCA model	Porosity	0.44	0.56	0.40	0.38	0.72
	Tortuosity	1.63	1.39	1.74	1.80	1.19
	Flow resistivity	30.797	25.376	36.313	33.641	36.989
	Thermal permeability (m <sup>2</sup> )	1.42E-09	1.53E-09	1.26E-09	1.39E-09	9.14E-10
	Viscous characteristic length (mm)	0.112	0.112	0.10863	0.116	8.95E-05
	Thermal characteristic length (mm)	0.166	0.171	0.156807	0.165	0.139
DB model	Flow resistivity (kPa · s/m <sup>2</sup> )	54.128	18.501	83.650	88.727	21.968
Miki model	Porosity	0.52	0.65	0.38	0.37	0.59
	Tortuosity	1.66	1.42	1.49	1.59	1.95
	Flow resistivity (kPa · s/m <sup>2</sup> )	10.590	11.663	10.792	9.147	12.758

Table 5.1: Physical and Extracted Parameters of Each Sample

## **CHAPTER 6**

### **CONCLUSION**

#### **6.0.1 Future Work**

Performing additional experiments on thicker grass substrate samples. The flow resistivity measurement system was not sensitive enough to record pressures for dried samples.

## BIBLIOGRAPHY

- [1] M. A. Biot. Mechanics of deformation and acoustic propagation in porous media. *Journal of Applied Physics*, 33(4):1482–1498, April 1962.
- [2] N. Dai, A. Vafidis, and E. R. Kanasevich. Wave propagation in heterogeneous, porous media: A velocity–stress, finite–difference method. *GEOPHYSICS*, 60(2):327–340, March 1995.
- [3] Kirill V. Horoshenkov, Amir Khan, and Hadj Benkreira. Acoustic properties of low growing plants. *The Journal of the Acoustical Society of America*, 133(5):2554–2565, 2013.
- [4] Jq Geertsma and D. C. Smit. Some aspects of elastic wave propagation in fluid-saturated porous solids. *Geophysics*, 26(2):169–181, 1961.
- [5] P. J. Dickinson and P. E. Doak. Measurements of the normal acoustic impedance of ground surfaces. *Journal of Sound and Vibration*, 13(3):309–322, November 1970.
- [6] R. J. Donato. Impedance models for grass–covered ground. *The Journal of the Acoustical Society of America*, 61(6):1449–1452, June 1977.
- [7] Keith Attenborough, Imran Bashir, and Shahram Taherzadeh. Excess attenuation and effective impedance associated with rough hard ground. *The Journal of the Acoustical Society of America*, 132(3):1903–1903, September 2012.
- [8] Bryan H. Song and J. Stuart Bolton. A transfer-matrix approach for estimating the characteristic impedance and wave numbers of limp and rigid porous materials. *The Journal of the Acoustical Society of America*, 107(3):1131–1152, 2000.
- [9] M. E. Delany and E. N. Bazley. Acoustical characteristics of fibrous absorbent material. *The Journal of the Acoustical Society of America*, 48(2A):434–434, August 2005.
- [10] David Linton Johnson, Joel Koplik, and Roger Dashen. Theory of dynamic permeability and tortuosity in fluid-saturated porous media. *Journal of Fluid Mechanics*, 176:379–402, 1987.
- [11] D. K. Wilson. Simple, relaxational models for the acoustical properties of porous media. *Applied Acoustics*, (3):171–188, 1997.



- [12] Yasushi Miki. Acoustical properties of porous materials-modifications of delany-bazley models. *J. Acoust. Soc. Jpn.(E)*, 11(1):19–24, 1990.
- [13] Yvan Champoux, Michael R. Stinson, and Gilles A. Daigle. Air-based system for the measurement of porosity. *The Journal of the Acoustical Society of America*, 89(2):910–916, 1991.
- [14] Denis Lafarge, Pavel Lemarinier, Jean F. Allard, and Viggo Tarnow. Dynamic compressibility of air in porous structures at audible frequencies. *The Journal of the Acoustical Society of America*, 102(4):1995–2006, October 1997.
- [15] M. E. Delany and E. N. Bazley. Acoustical properties of fibrous absorbent materials. *Applied Acoustics*, 3(2):105–116, April 1970.
- [16] Acoustics - determination of sound absorption coefficient and impedance in impedance tubes - part 2: Transfer function method.
- [17] J. Y. Chung and D. A. Blaser. Transfer function method of measuring induct acoustic properties. II. experiment. *The Journal of the Acoustical Society of America*, 68(3):914–921, September 1980.
- [18] J. Y. Chung and D. A. Blaser. Transfer function method of measuring induct acoustic properties. i. theory. *The Journal of the Acoustical Society of America*, 68(3):907–913, September 1980.
- [19] Keith Attenborough Olga Umnova. A cell model for the acoustical properties of packings of spheres. *Acta Acustica united with Acustica*, 87(2):226–235, 2001.
- [20] Olga Umnova, Keith Attenborough, and Kai Ming Li. Cell model calculations of dynamic drag parameters in packings of spheres. *The Journal of the Acoustical Society of America*, 107(6):3113–3119, June 2000.
- [21] E33 Committee. Test method for airflow resistance of acoustical materials. Technical report, ASTM International, 2003.